Generation and Kinetic Studies of Xe(5d[3/2]$_1$) Resonance State Atoms

V. A. Alekseev[†] **and D. W. Setser***

Department of Chemistry, Kansas State University, Manhattan, Kansas 66506

Received: April 22, 1999; In Final Form: August 16, 1999

Two-photon, pulsed-laser excitation of the Xe(4f[3/2]$_2$) level with concomitant amplified stimulated emission has been used to prepare the Xe(5d[3/2]$_1$) resonance state atoms in a few Torr of Xe. Observation of the vacuum ultraviolet emission at 119.2 nm from the Xe(5d[3/2]$_1$→5p^6 ^{1}S$_0$) transition permits direct monitoring of the decay rate of the concentration of the Xe(5d[3/2]$_1$) atoms, and the bimolecular quenching rate constants were measured at room temperature for Ar, Xe, CF_4, H_2, N_2, CO, CH_4, CCl_4, and Cl_2. The decay rate in Ne was too slow to measure and the decay mechanism in Kr was complex. The magnitudes of the quenching constants for Xe(5d[3/2]$_1$) atoms by molecules resemble those for the Xe(6s′[1/2]$_1$) and Xe(6p[1/2]$_0$ or [3/2]$_2$) states. In addition to introducing a slow quenching rate of the Xe(5d[3/2]$_1$) atoms, the addition of Ar to the cell containing a few Torr of Xe seemed to enhance the 119.2 nm emission intensity.

I. Introduction

Two-photon excitation of Xe and Kr atoms with concomitant amplified spontaneous emission (ASE) has been shown to be a simple and convenient method for time-resolved generation of their resonance-state[1,2] atoms in an environment suitable for kinetic studies. This method was used to generate the Xe(6s-[3/2]$_1$), Xe(6s′[1/2]$_1$), and Kr(5s[3/2]$_1$) resonance-state atoms and the quenching rate constants of those atoms were measured for a wide range of molecules.[1,2] In the present paper we report an extension of this method for the generation of Xe(5d[3/2]$_1$) resonance-state atoms using two-photon excitation of the Xe-(4f[3/2]$_2$) state. The energy levels of Xe are shown in Figure 1 for convenience of presentation. The 5d[3/2]$_1$ level is one of the upper states of the atomic xenon laser, which generates the 1.73 μm (5d[3/2]$_1$→6p[5/2]$_1$) transition and the 2.03 μm (5d-[3/2]$_1$→6p[3/2]$_1$) transition under particle beam excitation of Xe/Ar or Xe/Ar/He mixtures (see ref 3 and references therein). To the best of our knowledge, the quenching kinetics of Xe-(5d[3/2]$_1$) atoms have not been previously studied. In fact, little is known about the reactions of any of the states in the 5d manifold, because these states are difficult to selectively prepare and monitor.

An extensive study of the ASE following two-photon excitation of 6p′, 7p, 8p, and 4f states in Xe was reported by Miller.[4] Upon excitation of the 4f[3/2]$_2$ and 4f[5/2]$_2$ states, ASE transitions were observed for numerous transitions between levels in the 4f→5d, 6d→6p and 6p→6s manifolds. Transitions in the infrared between the 4f→6d levels and, perhaps, the 5d→6p levels, which were not observed in ref 4 because of the wavelength limitations of their detector, also could be expected. In particular, the 4f→6d ASE transitions should occur based upon observation of ASE from the 6d→6p transitions. The 4f-[3/2]$_2$ and 4f[5/2]$_2$ states are coupled by optical selection rules (directly to the d states or indirectly via cascade f→d→p→s transitions) with all resonance states of the Xe atom. The initial goal of the present work was to generate useful concentrations of Xe(5d[3/2]$_1$) and Xe(5d[1/2]$_1$) atoms using the ASE from

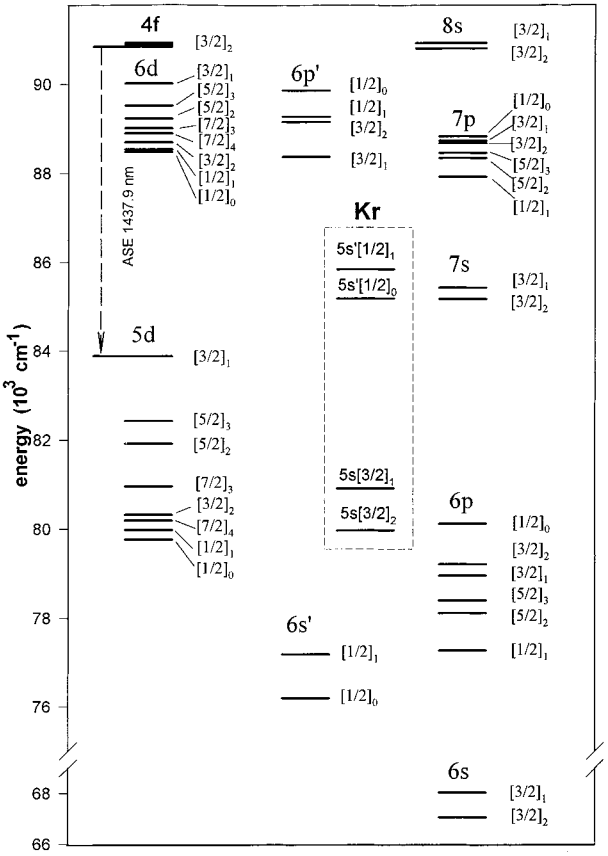

Figure 1. Energy level diagram for the excited states of Xe and Kr; the states are labeled in Racah notation. The lowest energy (91 169 cm^{-1}) Kr(5p) state, 5p[1/2]$_1$, is above the Xe(4f[3/2]$_2$) state (90 850 cm^{-1}).

two-photon excitation of the 4f states. We expected to observe the decay rates of the Xe(5d[3/2]$_1$) and Xe(5d[1/2]$_1$) atoms via their vacuum ultraviolet (vac UV) fluorescence at 119.2 and 125.0 nm, respectively, for subsequent kinetic studies. The 6s′-[1/2]$_1$ (129.6 nm) and 6s[3/2]$_1$(146.9 nm) resonance states, which already were studied earlier,[1] can be generated much more easily using two-photon excitation of the 6p′ and 6p states,

[†] Permanent address: Photonics Department, Institute of Physics, St. Petersburg University, 198904 St. Petersburg, Russia.

10.1021/jp991324g CCC: $18.00
Published on Web 10/04/1999

respectively. Emission from the 6d[3/2]$_1$ and 6d[1/2]$_1$ resonance states, 111.1 and 112.9 nm, is at too short a wavelength to be detected with our detection system. On the other hand, the 7s-[3/2]$_1$ resonance state at 117.0 nm could have, in principle, been observed. However, the complex ASE pathway leading to this state, 4f→6d→7p→7s, is apparently not feasible under our experimental conditions. On the basis of Miller's work,[4] two-photon pumping of the 7p or 8p states should lead more directly to generation of Xe(7s[3/2]$_1$) atoms via the ASE method.

In the present work, we report the generation of Xe(5d[3/2]$_1$) resonance state atoms from two-photon excitation of Xe-(4f) states with observation via the 119.2 nm emission intensity. The method is used to measure the quenching rate constants of Xe(5d[3/2]$_1$) atoms by Ar, Xe, H_2, N_2, CO, CH_4, CCl_4, CF_4, and Cl_2. The decay rate in Ne was too slow to measure, and preliminary experiments with Kr indicated a complex mechanism that involved populations in Xe^* levels above 5d[3/2]$_1$, as well as a slow quenching rate of the resonance atoms. The main point of the present study was to demonstrate that the ASE method could be used to generate and study Xe(5d[3/2]$_1$) atoms. We were not able to study the Xe(5d[1/2]$_1$) atoms because the 125.0 nm fluorescence was too weak. The difference between our ability to observe the 5d[1/2]$_1$ and 5d[3/2]$_1$ resonance atoms by fluorescence is discussed. Becasue of our limited resources, some interesting observations that were discovered will be noted, even though they could not be fully explored at this time.

II. Experimental Section

The experimental setup was described in refs 1 and 2, and we will present only a summary. The output from a Lambda Physik dye laser (LPD 3002) pumped by an XeCl laser (Questek 2840) was doubled by a BBO-II crystal to provide tunable ultraviolet laser pulses. Stilbene laser dye was used to obtain ~220 nm pulses for two-photon excitation of the Xe (4f) states. The laser pulse had a full-width at half-maximum of ~15 ns and the energy was ~ 0.1 mJ per pulse, as measured with a Precision power meter (model RJP-735). The dye laser was operated without an etalon, and the bandwidth of the second harmonic was 22 GHz. The experiments were performed in a stainless steel cell with 25 cm-long baffle arms. The cell was attached to the entrance flange of a 0.25 m Acton Research monochromator, which has a single optical surface. The cell was equipped with a LiF window for observation of the vac UV emission. The focused laser beam used to excite the Xe-(4f) states was directed 2−3 mm away from the lithium fluoride window. The monochromator was equipped with a 1200 g/mm concave grating blazed at 120 nm and a Hamamatsu R1220 solar blind photomultiplier tube, which has a 115−200 nm range for response. The ASE in the forward direction could be monitored with a 0.3 m McPherson monochromator equipped with a R955 Hamamatsu photomultiplier tube; a filter was used in front of the entrance slit of the McPherson monochromator to cut the UV laser light. The output signals of the R1220 and R955 Hamamatsu photomultiplier tubes were digitized with a Hewlett-Packard 54510A digital storage oscilloscope and transferred to a computer for storage and analysis. Unfortunately, the sensitivity of the R955 photomultiplier tube is very poor above 850 nm, and we were unable to observe several ASE transitions in the infrared region that would have been useful for a more complete interpretation of the nonlinear processes in these experiments.

Research grade Xe was obtained from Spectra Gases with a stated purity of 99.999%. Krypton of similar purity also was obtained from Spectra Gases. The molecular reagents were the standard reagent purity supplied by Matheson Gas Co. The pressures in the cell were measured by a Baratron pressure transducer attached directly to the laser cell. Experiments were performed by first adding Xe to the cell and then adding the reagent gas. Sufficient time for gas mixing in the cell was allowed before an experiment was started.

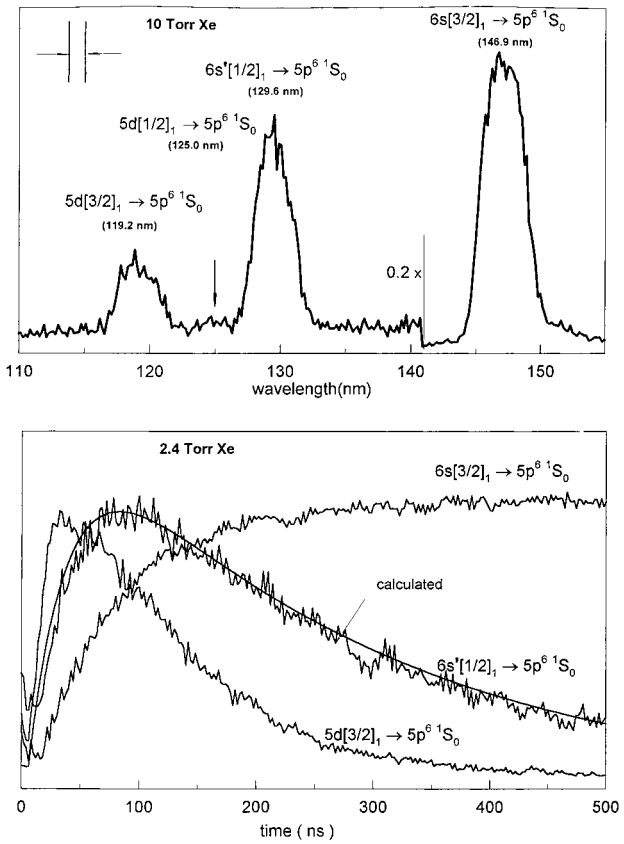

Figure 2. (top) Vac UV spectrum from 10 Torr of pure Xe under two-photon excitation of the Xe(4f[3/2]$_2$) state with focused laser radiation of ~0.1 mJ per pulse; note the change in scale for the 146.9 nm emission. (bottom) Waveforms for the three Xe resonance emission lines observed from 2.4 Torr of Xe. A simulated waveform for the Xe(6s′[1/2]$_1$→5p^6 ^{1}S$_0$) resonance line at 129.6 nm for the mechanism given in the text is shown by the solid curve.

III. Experimental Results

Vac UV Emissions Following Xe(4f[3/2]$_2$) Excitation. A typical fluorescence spectrum following two-photon pumping of the 4f[3/2]$_2$ state at 220.07 nm in 10 Torr of Xe is shown in Figure 2a. Of the possible five resonance transitions of Xe that are covered with our detection system, we observed emission from 5d[3/2]$_1$, 6s′[1/2]$_1$, and 6s[3/2]$_1$ atoms. Very weak emission at 125.0 nm from 5d[1/2]$_1$ may be present in the spectrum shown in Figure 2a, but the intensity was never strong enough to be useful. Excitation to the 4f[5/2]$_2$ state at 219.93 nm gave a similar spectrum, but the vac UV emission intensity was lower and all experiments to be reported were performed by pumping the 4f[3/2]$_2$ state. The 119.2 nm resonance emission is not particularly strong, but the intensity is adequate for kinetic studies. Although the 4f[3/2]$_2$→5d[1/2]$_1$ ASE transition at 920.3 nm was reported in ref 4, we were unable to observe significant 5d[1/2]$_1$→5p^6 ^{1}S$_0$ resonance emission intensity at 125.0 nm in any of our experiments. The apparent absence of the 5d[1/2]$_1$→5p^6 ^{1}S$_0$ emission is associated with the weak oscillator strength[5,6] of this transition, $f = 7.7 \times 10^{-3}$ vs $f = 1.1$ for 5d-[3/2]$_1$→5p^6 ^{1}S$_0$ and $f = 0.31$ for 6s′[1/2]$_1$→5p^6 ^{1}S$_0$. The 5d[1/

$2]_1$-$5p^6$ $^1S_0$ oscillator strength corresponds to an intrinsic radiative lifetime of 67 ns, which would be lengthened by a factor of approximately 10^3 by radiative trapping.[6] Thus, the vac UV radiative decay pathway cannot compete with the 5d-$[1/2]_1$-6p radiative transitions, which has a decay time of 3−4 μs to all 6p states. The intrinsic weakness of the $5d[1/2]_1 \rightarrow 5p^6$ $^1S_0$ transition also is evident from the absorption and fluorescence excitation spectra of gaseous Xe using synchtron radiation.[7] Another resonance emission that was not observed in our experiments is the $7s[3/2]_1 \rightarrow 5p^6$ $^1S_0$ transition at 117 nm. This transition is also weak, $f = 5.4 \times 10^{-2}$, and an alternative 7s→6p radiative pathway exists. The absence of the 117 nm emission could be due to the complexity of the ASE cascade pathway, 4f→6d→7p→7s, which prevented formation of the Xe($7s[3/2]_1$) atoms, or because of the difficulty of detection. Furthermore, the radiative transition rates from the 6p′ and 7p levels to the 7s levels are too small to provide an effective population transfer mechanism in the absence of ASE, in contrast to the mechanism proposed below to explain formation of Xe(6s′) resonance atoms.

In our previous studies of the Xe(6s), Xe(6s′), and Kr(5) resonance states, the build-up of concentration in the resonance state occurred within the ASE pulse, which has a similar time profile to that of the pumping laser pulse. That is, spontaneous radiative cascade processes did not contribute significantly to the concentrations of the resonance atoms. The waveforms of the 119.2, 129.6, and 146.9 nm emissions (Figure 2b) from the present experiments show that only the $5d[3/2]_1$ state seems to be directly generated by an ASE process; the other two have delayed rise times. We were unable to verify this conclusion by directly monitoring the ASE signals, because the $4f[3/2]_2 \rightarrow 5d[3/2]_1$ transition at 1437.9 nm could not be detected with a R955 PMT. On the basis of the rise time of the 119.2 nm signal, the growth of population in the $5d[3/2]_1$ state was $\sim 6 \times 10^7$ s^{-1}, which is consistent with formation by ASE during the laser pulse. The rates of growth of population in the 6s′ state, $\sim 3 \times 10^7$ s^{-1}, and in the 6s state, $\sim 1 \times 10^7$ s^{-1}, are significantly slower, which suggests involvement of collisional and/or spontaneous radiative decay processes in the formation mechanisms of the 6s and 6s′ atoms. The 6s′ emission intensity, relative to the 119.6 nm intensity, was reduced by a factor of 2 upon lowering the pressure from 10 to 2 Torr. Thus, collisions definitely are a factor in the Xe(6s′) formation mechanism.

Emission from $6s'[1/2]_1$ atoms was not observed in experiments using synchrotron radiation for direct one-photon excitation of $5d[3/2]_1$ atoms in pure Xe.[7a,b] We can conclude that the populations in the 6p states that are *radiatively coupled* to the $5d[3/2]_1$ level are not collisionally transferred to the 6s′ levels for our range of pressure,[7d] and states other than 6p and 5d levels must be involved in the mechanism of 6s′ formation by two-photon pumping of $4f[3/2]_2$. The most feasible mechanism seems to be one with three steps: (1) 4f→6d population transfer due to ASE, (2) collisional mixing of the Xe(6d, 6p′,7p) populations,[8] and (3) fast radiative decay from Xe(6p′) levels to Xe($6s'[1/2]_1$). Computer simulation of the time profile for the 129.6 nm resonance emission showed that the above model could satisfactorily fit the experimental profile (see Figure 2b). In the calculation, the rate for buildup of the concentration in the 6p′ states was taken the same as for the ASE generated 5d-$[3/2]_1$ state, 6×10^7 s^{-1}, and the rate for the 6p′→6s′ radiation transfer was taken to be the same as the total deactivation rate for the Xe(6p′) atoms at the given pressure, $\tau^{-1} + k_Q[\mathrm{Xe}] \approx 0.7.7 \times 10^7$ s^{-1} at 2.4 Torr of Xe, where $\tau = 40 \pm 5$ ns is the radiative lifetime of Xe(6p′) and $k_Q \approx 5 \times 10^{-10}$ cm^3 s^{-1} is the quenching rate constant.[8] The loss rate of $6s'[1/2]_1$ atoms was taken to be compatible with the direct excitation experiments of ref 1. The weakest point of the proposed mechanism is the required large rate for collisional transfer of population from the 6d levels to the 6p′ levels. Since the 6d levels have ∼70 ns lifetimes, the expected rate constants[8] of $\sim 5 \times 10^{-10}$ cm^3 s^{-1} will cause considerable collisional redistribution. The main question is whether the Xe(6p′) levels are the main products. Since the ASE is expected[4] to give populations in the $5d[3/2]_2$ and $6d[1/2]_1$ levels, and since the $6p'[3/2]_1$ level has nearly the same energy (see Figure 1), fast collisional transfer to the lowest energy 6p′ level may occur. More detailed consideration of the mechanism for $6s'[1/2]_1$ state formation would require observation of the ASE and spontaneous transitions in the infrared between numerous atomic states below the two-photon pumped state. Such a study was beyond the scope of the present paper.

The formation rate of the Xe(6s) resonance-state concentration seems to correlate with the decay rates of the $5d[3/2]_1$ and 6s′-$[1/2]_1$ concentrations. The radiative and collisional decay of the $5d[3/2]_1$ and $[1/2]_1$ concentrations will populate Xe(6p) levels that feed the $6s[3/2]_1$ state. The main decay process for Xe-($6s'[1/2]_1$) atoms, after the termination of the laser pulse, is collisional transfer to the $6p[1/2]_1$ state, which subsequently radiates to the $6s[3/2]_{1,2}$ levels.[1] The latter is the slowest process that contributes to formation of Xe($6s[1/2]_1$) atoms. We did not calibrate the wavelength response function of the Acton monochromator, but it certainly has considerably less sensitivity at the shorter wavelengths. Thus, the relative populations are consistent with formation of the $6s[3/2]_1$ concentration from collisional and radiative decay of the other two resonance states.

Decay Kinetics of Xe($5d[3/2]_1$) Atoms in Xe/Rg Mixtures. For a pressure range in which three-body processes can be neglected, the decay rate of the Xe($5d[3/2]_1$) atoms after the termination of the laser pulse is expected to be a sum of three separate first-order decay rates.

$$\beta = \beta_0 + \beta_{IR} + k_Q[\mathrm{Rg}] \qquad (1)$$

The first term is the decay rate of the imprisoned vac UV radiation. The Holstein formulation for radiative trapping predicts a pressure region in which decay rate is constant and given by eq 2.[10]

$$\beta_0 = \frac{0.269}{\tau_0}\left(\frac{\lambda}{R}\right)^{1/2} \qquad (2)$$

R is a geometrical factor (distance between the laser beam and observation window), τ_0 is the natural lifetime of the transition and λ is its wavelength. Equation 2 gives $\beta_0 \sim 1 \times 10^6$ s^{-1} for $R \sim 3$ mm, $\tau_0 = 1.4$ ns[9], and $\lambda = 119.2$ nm. Considering the results obtained for the decay of Xe($6s[3/2]_1$) and Kr($5s[3/2]_1$) resonance emissions intensities,[1,2] we expect that $P_{Xe} \sim 1-10$ Torr is the pressure range for which the decay rate of the 5d-$[3/2]_1 \rightarrow 5p^6$ $^1S_0$ imprisoned radiation is a constant as given by eq 2. The second term in eq 1 is the decay rate due to radiative transitions to the $6p[1/2]_1$, $6p[5/2]_2$, $6p[3/2]_1$, and $6p[3/2]_2$ states. The decay rates for these transitions are 4.0×10^4, 3.0×10^5, 2.5×10^6, and 6.0×10^3 s^{-1}, respectively,[5] which gives 2.8×10^6 s^{-1} for the total $5d[3/2]_1 \rightarrow 6p$ decay rate. The third term in eq 1 is the total rate of collisional relaxation to lower energy Xe levels.

Equation 1 is based on the assumption that all Xe($5d[3/2]_1$ formation processes will occur during the laser pulse. The data to be presented show that this is not necessarily the case for modest to high pressure of added rare gases. The decay profiles

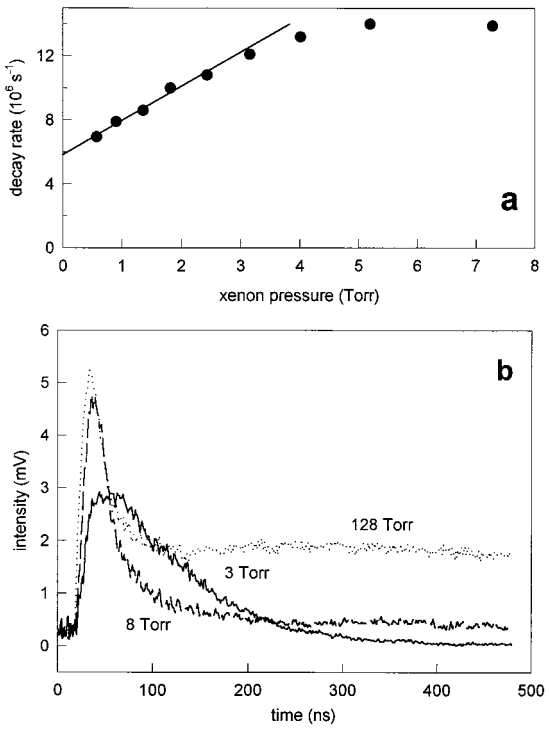

Figure 3. (a) Plot of the first-order decay constant of Xe(5d[3/2]$_1$) atoms vs xenon pressure. (b) Waveforms of the Xe(5d[3/2]$_1$→5p^6 ^{1}S$_0$) emission intensity for several Xe pressures.

in Xe were single exponential for pressures < 5 Torr. The first-order constants were measured from these profiles and a plot of these decay constants vs Xe pressure is shown in Figure 3a. Data from two independent experiments for the P_{Xe} < 5 Torr regime give an apparent rate constant for two-body quenching of Xe(5d[3/2]$_1$) atoms of 5.5×10^{-11} cm^3 s^{-1}. The average value for the intercept of this plot was 5.5×10^6 s^{-1}, which is in satisfactory agreement with the predicted value, $\beta_0 + \beta_{IR} = 3.8 \times 10^6$ s^{-1}, since β_0 and β_{IR} both have considerable uncertainty. The two-body rate constant by Xe is similar to rate constants for quenching of Xe(6p) states, and the product states presumably are lower energy Xe(5d or 6p) levels formed by interaction of the entrance and exit channel Xe^*_2 potentials.

A second, much slower, decay component appears in the decay profiles of Xe(5d[3/2]$_1$) atoms shown in Figure 3b from higher Xe pressure experiments. The apparent slow decay is probably a consequence of formation of Xe(5d[3/2]$_1$) atoms from a long-lived intermediate species. A likely mechanism is dissociative recombination of Xe_2^+ with an electron, which gives a distribution of Xe* states with a significant branching fraction for formation of Xe(5d) levels.[11,12] The Xe_2^+ ions can be formed by (i) three-photon ionization of Xe atoms followed by three-body association

$$Xe^+ + Xe + Xe \rightarrow Xe_2^+ + Xe \qquad (3)$$

or (ii) two-body associative-ionization collisions of Xe(4f[3/2]$_2$)

$$Xe(4f[3/2]_2) + Xe \rightarrow Xe_2^+ + e^- \qquad (4)$$

or (iii) energy-pooling ionization by collisions of two excited states of Xe*. The latter possibility has been discussed in studies of two-photon excitation of Xe(6p) states.[11] In the present experiments, the associative ionization reaction probably plays

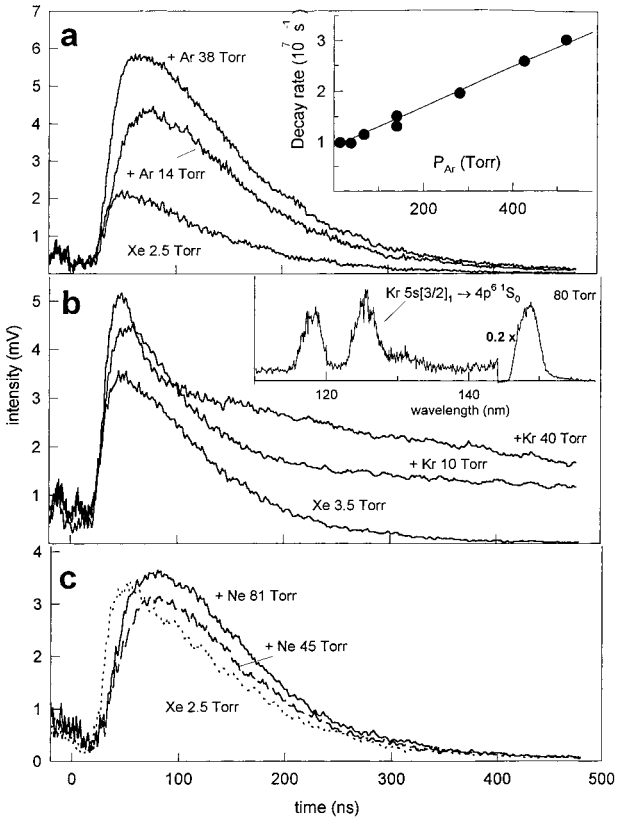

Figure 4. (a) Waveforms of the Xe(5d[3/2]$_1$→5p^6 ^{1}S$_0$) emission intensity for a fixed Xe pressure of 2.5 Torr with 14 and 38 Torr of Ar. The insert displays a plot of the first-order decay constant for Xe(5d[3/2]$_1$) atoms vs the pressure of Ar. (b) Waveforms of Xe(5d[3/2]$_1$→5p^6 ^{1}S$_0$) emission for a Xe pressure of 3.5 Torr with 10 and 40 Torr of Kr. The inset displays the vac UV emission spectrum of Xe (3.5 Torr) + Kr (80 Torr) mixture obtained from excitation of the Xe(4f[3/2]$_2$) state. (c) Waveforms of Xe(5d[3/2]$_1$→5p^6 ^{1}S$_0$) emission for 2.5 Torr of Xe with 45 and 81 Torr of Ne.

the major role since the 4f[3/2]$_2$ energy is above the threshold for Xe_2^+ formation (90 150 cm^{-1}).[13,14]

We performed preliminary experiments to investigate the influence of Ne, Ar, and Kr on the decay rate of 5d[3/2]$_1$ atoms, and some results are shown in Figure 4. The addition of ≤ 80 Torr of Ne hardly affected either the emission intensity or the decay rate of Xe(5d[3/2]$_1$) atoms (see Figure 4c), and the two-body quenching constant is less than $\sim 6 \times 10^{-13}$ cm^3 molecule^{-1} s^{-1}. The relatively high pressure of Ne did change the rise time and the position of the maximum signal presumably because of collisional effects with populations in high lying Xe* states. The addition of Ar caused a slow quenching of Xe(5d[3/2]$_1$) atoms and a remarkable augmentation of the 119.2 nm emission intensity (see Figure 4a). The growth in intensity occurs for P_{Ar} < 20 Torr; higher pressures of Ar result only in faster decay rates of the Xe(5d[3/2]$_1$) atoms with no noticeable change in the peak emission intensity. It is noteworthy that the position of the maximum of the time profile (Figure 4a and c) does shift to slightly later times with addition of Ar. This shift implies that some population is transferred to the 5d[3/2]$_1$ level by collisions involving Ar. The strong enhancement of the emission intensity by modest Ar pressure is of interest for further study. Considering the limited experimental data obtained in the present work, we can only mention here some processes that could be responsible for the enhancement of the Xe(5d[3/2]$_1$) emission intensity. (i) The intensity is proportional to the fraction, $\beta_0/(\beta_0 + \beta_{IR})$, of the Xe(5d[3/2]$_1$) atoms that emit in the vac UV (see eq 1). Collisional broadening of the Xe(5d[3/

$2]_1 \rightarrow 5p^6\ ^1S_0$) resonance line could result in an increased release of trapped radiation from the cell or, in other words, an increase in β_0 that would lead to a growth of vac UV intensity at the expense of the 5d→6p intensity. We observed a similar enhancement of Xe($6s[3/2]_1$) resonance emission upon addition of 3−30 Torr of CF_4 to a few Torr of Xe.[1] (ii) Enhancement of the $4f[3/2]_2 \leftarrow 5p^6\ ^1S_0$ two-photon cross-section due to collisional broadening of the absorption line. (iii) Collisional transfer of population from high-lying Xe* states to the $5d[3/2]_1$ state, including any residual population in the $4f[3/2]_2$ level that was not completely depleted by ASE. For example, Ar collisions might interfere with the processes that give the Xe($6s'[1/2]_1$) concentration. Such collisional effects probably are responsible for the shift of the maximum in the decay profiles with added Ne and Ar. (iv) Redistribution of intensity between various $4f[3/2]_2 \rightarrow 6d$ and $4f[3/2]_2 \rightarrow 5d$ ASE transitions and stimulated electronic Raman scattering (SERS) channels in favor of the $4f[3/2]_2 \rightarrow 5d[3/2]_1$ ASE channel.[1,4] Since SERS competes with ASE, the ability of the latter to transfer concentrations from one atomic state to another can be changed. Unlike ASE, development of the SERS requires fulfillment of certain phase-matching conditions between the laser and self-generated optical beams. Phase-matching can be affected by the dispersion of the gas media which, in turn, depends on pressure and composition. In our particular case, adding Ar could create an unfavorable dispersion environment for the development of SERS and, thus, enhance the concentration of Xe($5d[3/2]_1$) atoms in the cell.

The decay profiles in Xe/Kr mixtures resemble those from pure Xe in that a second slow decay component (Figure 4b) exists for modest pressures of Kr, as well as a fast component associated with collisional quenching of the $5d[3/2]_1$ atoms. Although the faster decay component is less obvious and more difficult to analyze than in pure Xe, the quenching rate by Kr seems to be slower than for Xe. The addition of Kr also removes the Xe($6s'[1/2]_1$) atoms by interfering with their formation process, and results in formation of the Kr($5s[3/2]_1$) resonance state, as shown by the inset in Figure 4b. The mechanism responsible for the long-term decay component may involve formation of Xe($5d[3/2]_1$) atoms from dimer ions; however, the threshold for Xe* + Kr associative ionization,[13] 94900 cm^{-1}, is well above the Xe(4f) energy. Three-photon ionization of Xe followed by three-body recombination could be responsible for $XeKr^+$ formation; however, the laser pulse energy was not high and probably does not produce the required concentration of Xe^+ ions. Other possibilities involve excitation−transfer mechanisms. Collisions between excited Xe* atoms with energy above 88 000 cm^{-1} and Kr atoms probably give Kr($5s'$) atoms as a product, and these atoms can yield Xe($5d[3/2]_1$) atoms by subsequent collision processes.[15] Another possibility is associative ionization from interaction of an excited Xe* atom with an excited Kr* atom. The $XeKr^+$ ion then could recombine with an electron to give a Xe(5d) atom.

Quenching Rate Constants for Xe($5d[3/2]_1$) Atoms by Molecules. Quenching rate constants for Xe($5d[3/2]_1$) atoms by seven molecular reagents were measured in the present experiments to demonstrate the applicability of the method for systematic measurement of quenching rate constants. Those experiments were done using two-photon excitation of $4f[3/2]_2$ at a constant xenon pressure of ~ 3 Torr plus variable pressure of molecular reagent gases. The pressures of the reagent gases were sufficiently low that the formation rate of Xe($5d[3/2]_1$) atoms was not affected, and eq 1 with an added quenching term applies. The waveforms for the decay of the 119.2 nm emission were single exponential, although the signal-to-noise ratio was somewhat limited, owing to the low response of our detection system at 119 nm. Three representative waveforms used to establish the quenching rate constant for N_2 are shown in Figure 5a. The Stern−Volmer plots of the pseudo first-order constants vs pressure for N_2, CO, and CH_4 molecules are shown in Figure 5b to illustrate the quality of our data. The quenching rate constants for $5d[3/2]_1$ atoms are listed in Table 1. The uncertainty of these rate constants is estimated as ±20%. The reliability is less than for our other ASE-based quenching studies[1,2] of Xe and Kr resonance states because of the low $5d[3/2]_1$ emission intensity from experiments at higher concentrations of reagent. To the best of our knowledge, no other data for the quenching of 5d states are available for comparison. We did not attempt to identify products from the reactions of

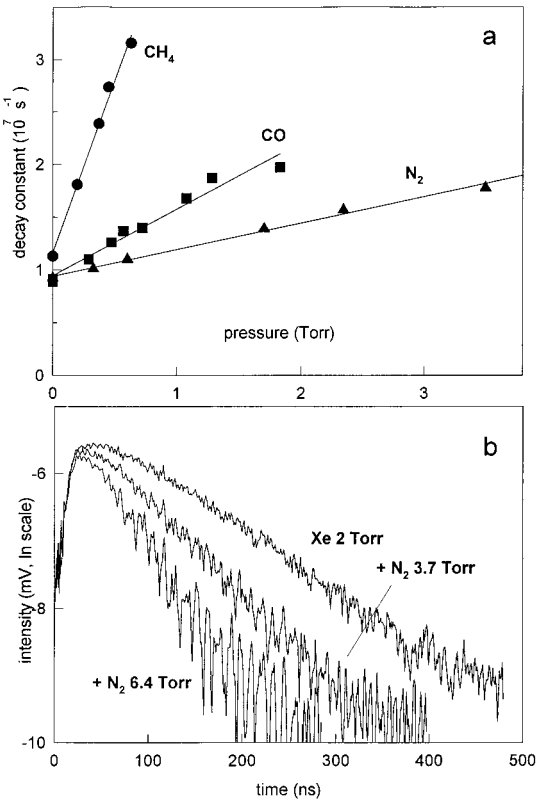

Figure 5. (a) Stern−Volmer plots of the first-order decay constants of Xe($5d[3/2]_1$) atoms vs CH_4, N_2, and CO pressures. (b) Waveforms of the Xe ($5d[3/2]_1 \rightarrow 5p^6\ ^1S_0$) emission intensity (log scale) used to obtain the first-order decay constant of Xe($5d[3/2]_1$) atoms in N_2.

TABLE 1: Quenching Rate Constants (10^{-10} cm^3 s^{-1}) for the $5d[3/2]_1$, $6p[3/2]_1$,$6s'[1/2]_1$, and $7p[5/2]_2$ States of Xe

	$5d[3/2]_1$ (this work)	$6s[3/2]_1$ (ref 1)[a]	$6s'[1/2]_1$ (ref 1)[a]	$6p[1/2]_0$ (ref 11)	$7p[5/2]_2$ (ref 8)
Ar	~0.01			1.4 ± 0.1	3.0 ± 0.6
Xe	0.55 ± 0.05		0.6	*b*	5.0 ± 0.5
N_2	0.78 ± 0.02	0.19	3.7	3.0 ± 0.3	
CO	2.0 ± 0.14	0.63	3.3	4.7 ± 0.5	9.9 ±1.5
H_2	2.6 ± 0.2	0.86		6.0 ± 0.8	4.5 ±0.5
CF_4	2.1 ± 0.2	0.03−0.06		2.8 ± 0.4	8.0 ± 0.4
CH_4	10.0 ± 0.5	3.3	10		30 ± 5
CCl_4	13.0 ± 0.8	7.8	8.1	7.5 ± 0.7	38 ± 4
Cl_2	11.0 ± 0.8	6.9	6.9	14.6 ± 1.5	37 ± 2

[a] The uncertainty in these measurements is ±5%, which is typical for the ASE[1,2] method. The larger uncertainty for the $5d[3/2]_1$ measurements is a consequence of the poorer signal-to-noise ratio for the 119.2 nm intensity. [b] The two-body quenching constant for Xe($6p[1/2]_0$) is anomalously small; however, the quenching constant for $6p[3/2]_2$ is 0.87×10^{-10} cm^3 s^{-1}.

Xe(5d[3/2]$_1$) atoms because the ASE generation technique produces several other excited Xe states, and reactions of all these excited atoms also give products.

Discussion

ASE Generation of the Xe(5d) Resonance States. The work presented here demonstrates that 5d[3/2]$_1$ atoms are generated in adequate concentrations for study by observation of their 119.2 nm fluorescence intensity following two-photon excitation of the 4f[3/2]$_2$ state in a few Torr of Xe. To avoid a secondary formation reaction, the pressure of Xe should be maintained below 5 Torr. The decay rate of the 5d[3/2]$_1$ atoms in Xe is faster than the predicted value from considering just the trapped vac UV radiation because of the 5d→6p alternative radiative decay pathway. An important question is why emission from the 5d[1/2]$_1$ state atoms was not observed under the same experimental conditions? Miller,[4] in fact, did observe the direct 4f[3/2]$_2$→5d[1/2]$_1$ ASE transition at 920.3 nm in his experiments, and 5d[1/2]$_1$ atoms should have been generated in our experiments. The simplest explanation for the inability to record the 125 nm fluorescence is the one offered by Castex et al.[6] to explain the absence of the 125 nm emission following one-photon excitation of the 5d[1/2]$_1$ state. Radiative trapping of the vac UV transition in a few Torr of Xe is expected to lengthen the free lifetime (~70 ns) by 2−3 orders of magnitude so that the 6d→6p radiative pathway ($\tau \approx 3\ \mu$s) becomes the dominant radiative decay route and, thus, the 125 nm fluorescence signal is very weak. Castex and co-workers also observed a slow quenching of Xe(5d[1/2]$_1$) atoms with added Xe pressure, which they assigned to a three-body process. This explanation must be balanced against the observation of the 125 nm fluorescence following two-photon excitation of 6p[1/2]$_0$ atoms in Xe/Ar mixtures.[16] Collisions with Ar (but not Xe) rapidly couple the populations in the 6p[1/2]$_0$ and 5d[1/2]$_1$ levels, which have an equilibrium constant of 0.18 at 300 K. The measured *effective* lifetime (110 ns)[16] obtained for 4 mTorr of Xe with extrapolation to zero Ar pressure corresponds to a Xe(5d[1/2]$_1$) lifetime of 200 ns, if the 6p[1/2]$_0$ and 5d[1/2]$_1$ levels are assumed to be collisionally coupled. The measured effective lifetime of the coupled levels decreased with increased Xe pressure (up to 3 Torr), which was interpreted as a large two-body quenching rate of Xe(5d[1/2]$_1$) atoms by Xe.[16] In fact, one might have expected a *lengthening* of the effective lifetime with increased Xe pressure because of enhanced radiation trapping. Interpretation of these observations could be further complicated by pressure broadening of the 125 nm emission line by the presence of Ar, as we found for the Xe(5d[3/2]$_1$) transition.

Several of the potentials for the Xe_2* molecular states that correlate to Xe(6p[1/2]$_0$) and Xe(5d[1/2]$_1$) have been characterized,[17] and this information has some utility for understanding the collisional quenching rates of the Xe(5d[1/2]$_1$) atoms. Six potentials correlate to the 6p[1/2]$_0$ and 5d[1/2]$_1$ states.[17−19] The 0_g^+ potentials correlating to 6p[1/2]$_0$ and 5d[1/2]$_1$ are only weakly predissociative and should not contribute toward two-body quenching. In fact, these potentials could support three-body quenching with excimer formation. However, the bound (1290 cm^{-1}) 1_g state correlating to the 5d[1/2]$_1$ limit is strongly predissociative during the 4 ns laser pulse. The assigned vibrational states in the 1_g potential are regular and, perhaps, the interactions are not so strong as to lead to two-body collisional mixing with a large rate constant. Two vac UV band systems[20,21] of Xe_2 have been identified in absorption that are close to the 5d[1/2]$_1$ energy. However, it is not possible to characterize the *u*-state potentials in sufficient detail to elucidate properties such as predissociation. Experiments to directly identify the collisional quenching properties of 5d[1/2]$_1$ atoms, which is the lowest energy 5d resonance state, are still needed to resolve the different claims in ref 6 and 16. More carefully designed two-photon ASE experiments might provide useful data. With a red-sensitive PM tube, the 4f[3/2]$_2$ or 4f[5/2]$_2$ ASE transitions to 5d[1/2]$_1$ could be monitored and conditions adjusted so that the concentration in the 5d[1/2]$_1$ level was optimized. Possibly the 125 nm signal then could be directly observed.

Our ASE experiments also resulted in the generation of Xe(6s[3/2]$_1$) and Xe(6s′[1/2]$_1$) atoms. However, the formation mechanism depended upon collision processes rather than direct ASE. As already explained, the Xe(6s) atoms seem to arise from radiative decay of the Xe(6s′[1/2]$_1$)−Xe(6p[1/2]$_1$) coupled pair plus radiative and collisional decay of the Xe(5d) states. The relatively strong emission from Xe(6s′) atoms was a surprise, since a radiative cascade pathway from 4f[3/2]$_2$ seems not to exist. A fast collisional coupling of the 6d[3/2]$_2$ and 6d[1/2]$_1$ states (formed by ASE) with the 6p′[3/2]$_1$ state was suggested. The 6p′[3/2]$_1$ atoms would radiate to 6s′[1/2]$_1$. Such collisional coupling has been observed in He gas,[22] but it would not necessarily be expected in Xe collisions, which tend to be less restrictive in terms of product states.[8,23,24] The elimination of the Xe(6s′) formation pathway by the addition of Kr also lends some support to the involvement of the Xe(6p′) states in the mechanism for Xe(6s′[1/2]$_1$) formation. The absence of Xe(6s[3/2]$_1$) formation in direct excitation[7] of Xe(5d[3/2]$_1$) also suggests a role for higher energy Xe* states in the formation mechanism.

Quenching of Xe(5d[3/2]$_1$) Atoms by Rare Gas Atoms. The 5d[3/2]$_1$ resonance atoms have a two-body quenching constant by Xe that is similar to those of Xe(6p) states (except for the very stable 6p[1/2]$_0$ level[16,23−25]). The magnitude of the quenching constant is consistent with the partly predissociated nature of the 1_g potential[17] that exists to the red side of the 5d[3/2]$_1$ energy limit. The photoelectron energy data from excitation of the shallow 1_g potential are consistent with predissociation to give the 5d[3/2]$_2$ state.[17] Three potentials with *u* symmetry that are near the 5d[3/2]$_1$ level also should be considered.[21] The Japanese group observed the excitation spectra of these *u* states by monitoring either the vac UV or red Xe(6p−6s) emission intensity, and predissociation could be either intramultiplet to lower 5d levels or intermultiplet to 6p levels.[21] Thus, collisional quenching pathways of Xe(5d[3/2]$_1$) atoms seem to exist by Xe_2* potentials of either *g* or *u* symmetry. Although the 5d[3/2]$_1$ level appears to be somewhat isolated in Figure 1, our data show that it is less stable to Xe collisions than the top level of the 6p manifold, and Xe(5d[3/2]$_1$) atoms are quenched by two-body Xe collisions.

As we already discussed, the slowly decaying 5d[3/2]$_1$ component that develops at higher Xe pressure probably is associated with a formation rate arising from electron recombination with Xe_2^+. The formation of Xe_2^+ can arise from associative ionization of the 4f[3/2]$_2$ atoms. A direct study of this process by pulsed excitation of Xe(4f[3/2]$_2$) atoms at low laser power where ASE does not exist is worthwhile and feasible.[4] Analysis of the Xe_2* potentials correlating to the 4f[3/2]$_2$ and/or 4f[5/2]$_2$ levels shows that both predissociation and autoionization occur.[14] The predissociation channels from Xe_2*(4f) potentials to the 6p′ levels offer another route for the formation of 6s′[1/2]$_1$ atoms, provided that the branching fraction for Xe(6p′) formation competes with associative ionization in Xe + Xe(4f[3/2]$_2$) collisions.

The quenching data in Kr gas are complex, and we made no effort to develop a mechanism. However, the two-body quenching rate of $5d[3/2]_1$ atoms by Kr must be slower than the rate for Xe. The $XeKr^*$ potentials correlating to $5d[3/2]_1$ have not yet been investigated. However, the correlation diagram suggests that the 0^+ and 1 potentials would be very weakly attractive and possibly rather isolated.[26] A slow decay (in reality a slow formation rate) develops for Kr pressures above 10 Torr. Two-body $5d[3/2]_1$ + Kr associative ionization to give $XeKr^+$ is not possible, since the threshold energy is too high. The Xe(4f, 6p′, 7p, and 6d) atoms will have large rate constants for excitation transfer to Kr in two-body collisions with probable formation of Kr(5s′) and or Xe(7s) atoms, which in turn may relax to Xe-$(5d[3/2]_1)$ atoms.[7] Keto and co-workers[25] attempted to characterize the energy flow from Xe(6p′,7p) atoms to Kr, but the mechanism is still not complete. However, a collisional mechanism involving just excited Xe^* atoms that would deliver Xe-$(5d[3/2]_1)$ atoms for such a long period seems difficult to formulate. An alternative possibility is associative ionization giving $XeKr^+$ from collisions of excited Xe^* atoms with excited Kr^* atoms. Some mechanism in Kr buffer gas clearly exists that provides high concentrations of excited Xe^* states for some time, and this phenomenon merits further study.

In contrast to the top level of the Xe(6p) manifold, the Xe-$(5d[3/2]_1)$ level is rather stable to collisions with Ar and Ne (and probably He). The calculated potentials for $Xe(5d[3/2]_1)$−Ar and $Xe(5d[3/2]_1)$−He seem to be repulsive and isolated.[27] These results may be relevant for building up populations in the Xe(5d) manifold in discharge devices involving Xe in modest pressures of He, Ne, or Ar. At very high pressure of Ar (70 bar) the $5d[3/2]_1$ state is quenched.[7c]

Quenching Rate Constants for Xe(5d[3/2]$_1$) Atoms by Molecules. The quenching rate constants for Xe(6s, 6s′, 6p, and 7p) state atoms are compared to those for $Xe(5d[3/2]_1)$ in Table 1. The rate constants for the $5d[3/2]_1$ atoms are consistently smaller than those for $7p[5/2]_2$ atoms and larger than those for $6s[3/2]_1$ atoms. Except for N_2, the rate constants for $5d[3/2]_1$ atoms are comparable to those for 6p or 6s′ atoms. Although the energy of the $5d[3/2]_1$ atoms is 4000 cm^{-1} above that of the 6p levels, the reactive cross-sections actually are slightly smaller than those of the 6p atoms. Excited-state Cs atoms can serve as a model for Xe atoms. The computed polarizabilities of Cs atoms[28] indicate that the 5d state has a 3-fold smaller polarizability than the 6p state; however, the effective quantum numbers are similar.[28] Thus, the slightly larger, on average, rate constants for the Xe(6p) atoms vs $Xe(5d[3/2]_1)$ atoms are understandable. It also should be remembered that the $J = 0$ and 1 states of the Xe(5d) manifold are intrinsically mixed with the Xe(6s′) states of the same J.[27,29] The reagents in Table 1 represent three types of reaction mechanisms. For Ar and Xe, the products must be other excited states of Xe. For N_2 and CO, the products will be bound excited states of CO and N_2;[11,30] the mechanism also is excitation transfer for CH_4 and CF_4, but to dissociative molecular states. The dominant pathway for Cl_2 and CCl_4 is reactive quenching.[8,11] The mechanism for H_2 is not established; quenching could occur by excitation transfer and/or reactive quenching, as found for excited states of Cs atoms. The latter involves the $V(Cs^+, H_2^-)$ potential.[31] Only excited states of XeH are bound and such emission was not observed from quenching of Xe(6p′,7p) atoms.[8]

Conclusions

Two-photon, pulsed-laser excitation to the $Xe(4f[3/2]_2)$ level with ASE has been shown to be a useful way to generate Xe-$(5d[3/2]_1)$ atoms for subsequent kinetic study. Although the ASE transition between the 4f and 5d levels could not be observed, the rise time for the formation of $Xe(5d[3/2]_1)$ atoms strongly suggests that the mechanism of formation is ASE. On the basis of representative reagent molecules, the room-temperature quenching rate constants for $Xe(5d[3/2]_1)$ atoms by molecules seem to be comparable to or slightly smaller than those of Xe-(6p) atoms. The two-body quenching rate constants of Xe(5d-$[3/2]_1$) atoms by Ne, Ar, and Kr are quite small; however, Xe has a quenching rate constant of 5.5×10^{-11} cm^3 s^{-1}. (Note added in proof: These observations are consistent with a recently proposed model given in ref 32.) For Xe or Kr pressures above ~8 Torr, a very slow formation process for Xe(5d[3/$2]_1$) atoms develops in addition to the fast ASE pathway. At least in Xe buffer, the slow process may be electron recombination with Xe_2^+ ions. Several questions involving the kinetics of excited states of Xe^* were identified in these experiments that merit additional study. One such item is the verification of the suggestion for why the $Xe(5d[1/2]_1)$ resonance state atoms were not observed, even though they probably were prepared by the ASE pulse.

Acknowledgment. This work was supported by the U.S. National Science Foundation, CHE-9505032. We thank Dr. Wayne Danen of the Los Alamos National Laboratory for arranging the loan of the vacuum ultraviolet monochromator that made these experiments possible.

References and Notes

(1) Alekseev, V. A.; Setser, D. W. *J. Chem. Phys.* **1996**, *105*, 4613.

(2) Alekseev, V. A.; Setser, D. W. *J. Phys. Chem. A* **1999**, *103*, 4016.

(3) (a) Alford, W. J.; Hays, G. N.; Ohwa, M.; Kushner, M. J. *J. Appl. Phys.* **1990**, *69*, 1843. (b) Kurochin, V. Yu.; Udalov, Yu. B.; Tskhai, S. N.; Blok, F. J.; Peters, P. J. M.; Witteman, W. J.; Petrovskij, V. N.; Protsenko, E. D. *Appl. Phys. B* **1997**, *65*, 37.

(4) Miller, J. C. *Phys. Rev. A* **1989**, *40*, 6969.

(5) Aymar, M.; Coulombe, M. *At. Data Nucl. Data Tables* **1978**, *21*, 537.

(6) Museur, L.; Kanaev, A. V.; Zheng, W. Q.; Castex, M. C. *J. Chem. Phys.* **1994**, *101*, 10548.

(7) (a) Brodman, R.; Zimmerer, G. *Chem. Phys. Lett.* **1978**, *56*, 434. (b) Brodman, R.; Zimmerer, G.; Hahnm, U. *Chem. Phys. Lett.* **1976**, *41*, 160. (c) Laporte, P.; Subtil, J. L.; Reininger, R.; Gurtler, P. *Chem. Phys.* **1993**, *177*, 257. (d) This conclusion also is in accord with current understanding of two-body relation mechanism of Xe(6p) states in Xe buffer gas. See ref 23−25.

(8) Alekseev, V. A.; Setser, D. W. *J. Phys. Chem.* **1996**, *100*, 5766.

(9) Matthias, E.; Rosenberg, R. A.; Poliakoff, E. D.; White, M. G.; Lee, S. T.; Shirley, D. A. *Chem. Phys. Lett.* **1977**, *52*, 239.

(10) (a) Holstein, T. *Phys. Rev.* **1947**, *72*, 1212; **1951**, *83*, 1159. (b) Lawler, J. E.; Curry, J. W. *J. Phys. D* **1998**, *31*, 1.

(11) Nelson, T. O.; Setser, D. W.; Richman, M. K. *J. Phys. Chem.* **1995**, *99*, 7482.

(12) (a) Shiu, V. J.; Biondi, M. A.; Sipler, D. D. *Phys. Rev. A* **1977**, *15*, 494. (b) Kuo, C. Y.; Kotz, J. W. *J. Chem. Phys.* **1983**, *78*, 1851. (c) Xie, J.-B.; Kuo, B.; Lo, D. *J. Phys. B At. Mol. Opt. Phys.* **1991**, *24*, 300.

(13) Dehmer, P. M.; Pratt, S. T. Vac UV Spectroscopy of Rare-Gas van der Waals Dimers in *Photophyiscs and Photochemistry in the Vacuum Ultraviolet*; McGlynn, S. P., Findley, G. L., Huebner, R. H., Eds.; NATO ASI Series C: Mathematical and Physical Sciences, **1982**, *142*, 467.

(14) (a) Huo, X. K.; Mao, D. M.; Shi, Y. J.; Dimov, S. S.; Lipson, R. H. *J. Chem. Phys.* **1998**, *109*, 3944. (b) Pratt, S. T.; Dehmer, P. M.; Dehmer, J. L. *Chem. Phys. Lett.* **1990**, *165*, 135.

(15) Sobczynski, R.; Setser, D. W. *J. Chem. Phys.* **1991**, *95*, 3310.

(16) Bruce, M. R.; Layne, W. G.; Whitehead, C. A.; Keto, J. W. *J. Chem. Phys.* **1990**, *92*, 2917.

(17) Hu, X. K.; Mao, D. M.; Dimov, S. S.; Lipson, R. H. *J. Chem. Phys.* **1997**, 106, 9411, 9419.

(18) (a) Hu, X. K.; Mao, D. M.; Dimov, S. S.; Lipson, R. H. *Phys. Rev. A* **1996**, *54*, 2814. (b) Hu, X. K.; Mao, D. M.; Dimov, S. S.; Lipson, R. H. *Chem. Phys.* **1995**, *201*, 557. (c) Dimov, S. S.; Cai, J. Y.; Lipson, R. H. *J. Chem. Phys.* **1994**, *101*, 10313.

(19) Keto, J. W.; Cai, H.; Kykta, M.; Lei, C.; Möller, T.; Zimmerer, G. J. Chem. Phys. **1997**, *107*, 6080.

(20) a) Castex, M. C.; Damany, N. *Chem. Phys. Lett.* **1972**, *13*, 158; **1974**, *24*, 437. (b) Castex, M. C. *Chem. Phys.* **1974**, *5*, 448.

(21) Tsukiyama, K.; Kasuya, T. *J. Mol. Spectrosc.* **1992**, *151*, 312.

(22) Zikratov, G.; Setser, D. W. *J. Chem. Phys.* **1996**, *104*, 2243.

(23) Xu, J.; Setser, D. W. *J. Chem. Phys.* **1990**, *92*, 4191.

(24) Alford, W. J. *J. Chem. Phys.* **1992**, *96*, 4330.

(25) Whitehead, C. A.; Pournasr, H.; Bruce, M. R.; Cai, H.; Kohel, J.; Layne, W. B.; Keto, W. *J. Chem. Phys.* **1995**, *102*, 1965.

(26) Lipson, R. N.; Dimov, S. S.; Hu, X. K.; Mao, D. M.; Cai, J. Y. *J. Chem. Phys.* **1995**, *103*, 6313.

(27) Hickman, A. P.; Huestis, D. L.; Saxon, R. P. *J. Chem. Phys.* **1992**, *96*, 2099.

(28) van Wijngaarden, W. A.; Li, J. *J. Quant. Spectrosc. Radiat. Transfer* **1994**, *52*, 555.

(29) Liberman, P. S. *J. de Phys.* **1969**, *30*, 53.

(30) (a) Zhong, D.; Setser, D. W. *Chem. Phys. Lett.* **1993**, *207*, 555. (b) Zhong, D.; Setser, D. W.; Sobczynski, R.; Gadomski, W. *J. Chem. Phys.* **1996**, *105*, 5020.

(31) (a) Huang, X.; Zhao, J.; Xing, G.; Wang, X.; Bersohn, R. *J. Chem. Phys.* **1996**, *104*, 1388. b. L'Hermitz, J. M. *J. Chem. Phys.* **1992**, *97*, 6215. (c) L'Hermitz, J. M.; Rahmat, G.; Vetter, R. *J. Chem. Phys.* **1991** *95*, 3347. (d) Fan, L.-H.; Chen, J. J.; Lin, Y.-Y.; Luh, W.-T. *J. Phys. Chem. A* **1999**, *103*, 1300.

(32) Mao, D. M.; Hu, X. K.; Shi, Y. J.; Lipson, R. H. *J. Chem. Phys.* **1999**, *111*, 2985.